

RESEARCH LETTER

10.1002/2015GL063865

Key Points:

- Satellite passive microwave data are used for polar low detection
- Usage of these data allows revealing polar lows covered by upper clouds
- Correlation between the number of polar lows and sea ice extent is examined

Correspondence to:
J. E. Smirnova,
jsmirnova@shuru

Citation:
Smirnova, J. E., P. A. Golubkin, L. P. Bobylev, E. V. Zabolotskikh, and B. Chapron (2015), Polar low climatology over the Nordic and Barents seas based on satellite passive microwave data, *Geophys. Res. Lett.*, 42, 5603–5609, doi:10.1002/2015GL063865.

Received 15 MAR 2015
Accepted 13 JUN 2015
Accepted article online 16 JUN 2015
Published online 6 JUL 2015

Polar low climatology over the Nordic and Barents seas based on satellite passive microwave data

Julia E. Smirnova¹, Pavel A. Golubkin¹, Leonid P. Bobylev^{2,3}, Elizaveta V. Zabolotskikh¹, and Bertrand Chapron^{1,4}

¹Satellite Oceanography Laboratory, Russian State Hydrometeorological University, St. Petersburg, Russia, ²Nansen International Environmental and Remote Sensing Centre, St. Petersburg, Russia, ³Nansen Environmental and Remote Sensing Centre, Bergen, Norway, ⁴Laboratoire d'Océanographie Spatiale, Institut Français de Recherche Pour L'exploitation de la Mer, Plouzané, France

Abstract A new climatology of polar lows over the Nordic and Barents seas for 14 seasons (1995/1996–2008/2009) is presented. For the first time in climatological studies of polar lows an approach based on satellite passive microwave data was adopted for polar low identification. A total of 637 polar lows were found in 14 extended winter seasons by combining total atmospheric water vapor content and sea surface wind speed fields retrieved from Special Sensor Microwave/Imager data. As derived, the polar low activity in the Norwegian and Barents Seas is found to be almost equal, and the main polar low genesis area is located northeastward of the North Cape. For the Barents Sea, a significant correlation is found between the number of polar lows and mean sea ice extent. Individual indicative polar low characteristics (i.e., diameter, lifetime, distance traveled, translation speed, and maximum wind speed) are also presented.

1. Introduction

Polar lows are intense mesoscale cyclones that are associated with cold air outbreaks and form poleward of the main baroclinic zone. Sometimes referred to as Arctic hurricanes, polar lows are short-lived (less than 48 h) and small-scale (less than 1000 km) cyclones, unlike their tropical counterparts. What they do have in common is strong surface winds: at least gale force is required for a polar low. These definition and set of criteria became conventional since their publication by Rasmussen and Turner [2003] and are used throughout this letter.

Given their short lifetime and small horizontal scales, polar lows are rarely spotted on weather charts, making difficult their early detection, monitoring, and especially compilation of some form of polar low climatology. One of the first climatological studies was published by Wilhelmsen [1985]. Statistics about polar lows near the Norwegian coast were obtained using weather maps, in situ observations, reports of shipwrecks, and a few satellite images. While mostly concentrated on the period 1978–1982, the total number of polar low events for 1972–1982 was reported to be 71.

Subsequent availability of more densely sampled satellite observations (i.e., infrared imagery) revealed a more frequent occurrence of these phenomena. Until the present day it is a common practice to utilize infrared imagery collected by radiometers on board polar orbiting satellites for polar low tracking. Blehschmidt [2008] used Advanced Very High Resolution Radiometer (AVHRR) data to monitor the 2004–2005 period. As reported, 90 polar lows were found (45 per year in average) over the Barents, Norwegian, Greenland, and Irminger Seas.

More recently, Noer et al. [2011] also used AVHRR infrared imagery along with model fields from the High Resolution Limited Area Model (HIRLAM) and from a version of the UK Met Office Unified Model. Polar lows, to be classified as such, were expected to meet additional requirements; i.e., certain meteorological conditions favorable for polar low development should be observed in the analyzed model data prior to polar low formation. Results of this study yield 121 cases over 10 years (2000–2009). Recently, the study period was extended to 2013 by Rojo et al. [2015], and resulting average number per year was reported to be 13.57.

Solely based on simulations of a local area model initialized by National Centers for Environmental Prediction/National Center for Atmospheric Research (NCEP/NCAR) reanalysis, Zahn and von Storch [2008] found 3313 polar lows during 1949–2005 in the North Atlantic, which corresponds to an annual mean of 56 cases (only 28 of which belong to the Nordic and Barents seas). Underrepresentation of polar lows in global atmospheric reanalyses might certainly be of concern for such analysis. Dedicated studies to

estimate the number of polar lows that may be tracked using reanalyses data [Zappa et al., 2014], including the case when these data are used as initial and lateral boundary conditions for simulations of nonhydrostatic model [Laffineur et al., 2014], report that at least 20% of events cannot be captured. This fraction might be larger since both Zappa et al. [2014] and Laffineur et al. [2014] used reference polar low data set derived from Noer et al. [2011] list, which contains considerably lower number of polar lows compared to, e.g., Bleckschmidt [2008] due to stricter criteria used for polar low selection.

The relevance of satellite passive microwave data for polar low research was demonstrated before in several case studies [e.g., Claud et al., 1993, 2004, 2009; Bobylev et al., 2011]. In these studies polar lows were detected through the subjective analysis of brightness temperatures (TBs) or geophysical parameters derived from TBs. However, to the best of our knowledge there have been no systematic and dedicated studies that adopted this approach to infer polar low climatology. This may be due to relatively low spatial resolution of microwave data (12.5–25 km) compared to infrared imagery (~1 km). Indeed, this resolution might be not high enough for regular investigation of polar low mesoscale features, but it is sufficient for determination of polar low occurrence per se. Moreover, microwave observations can be obtained under the cloud top to enable the detection of underlying polar lows undetectable by thermal infrared imagery [Bobylev et al., 2011].

In this study, atmospheric total water vapor (TW) content fields derived from Special Sensor Microwave/Imager (SSM/I) TBs are thus routinely searched for signatures that suggest the possible presence of a polar low, further corroborated by applying wind speed criterion. Hereafter, we present this new climatology of polar lows over the Nordic and Barents seas for 14 seasons (1995/1996–2008/2009) as compiled using this method.

2. Data and Methods

SSM/I instrument on board the Defense Meteorological Satellite Program (DMSP) series of satellites contains seven separate radiometers taking simultaneous measurements at 19.35, 37, 85.5 GHz frequencies in vertical and horizontal polarization and at 22.235 GHz in vertical polarization. The spatial resolution increases with higher frequency: 56 km for the 19.35 GHz, 45 km for the 22.235 GHz, 32.5 km for the 37 GHz, and 14 km for 85.5 GHz. Spatial sampling allows to obtain 25 km resolution for all channels with an exception of 85.5 GHz channel where resolution is increased to 12.5 km.

Brightness temperatures from SSM/I on board the DMSP F13 spacecraft were collected for the Nordic (i.e., Norwegian and Greenland) and Barents seas from September 1995 to April 2009. Measurements from five lower frequency channels were then taken to obtain atmospheric TW content fields with 25 km spatial resolution using a retrieval algorithm described in Bobylev et al. [2010]. This algorithm is tuned for the Arctic conditions, leading to a higher accuracy (retrieval error 1.34 kg m^{-2}) than the Wentz [1997] global operational algorithm (retrieval error 1.90 kg m^{-2}). This is especially important since TW content in polar lows can be just $2\text{--}3 \text{ kg m}^{-2}$ higher than in surrounding areas. Consistent polar low detection thus becomes impossible if the retrieval error is close to these values.

Obtained TW fields were further visually analyzed for the presence of polar low-like vortices which manifest themselves as a cyclonic signature having small horizontal extent and exceeding ambient level of the TW content by at least 2 kg m^{-2} . Then, the detected vortices were defined as polar lows only if sea surface wind speed exceeded 15 m s^{-1} as estimated using SSM/I wind products provided by Remote Sensing Systems (<http://www.remss.com>). Standard wind speed retrieval error of the algorithm used for these products is 0.9 m s^{-1} [Wentz, 1997]. Though this error is rather small, it may have an effect on selection of borderline cases with wind speeds near 15 m s^{-1} . Accounting for this, and also for growth of the error in unfavorable conditions (e.g., high cloud liquid water content), only a formed group of pixels with wind speeds above the threshold was considered. Both TW and wind speed fields were also checked for 3 days before the first and 3 days after the last observation of a vortex under consideration to exclude possibility of selection of synoptic systems into further analysis.

Additionally, presence of cloud signature on infrared imagery was checked for each detected polar low using AVHRR quicklook images from the Dundee Satellite Receiving Station (<http://www.sat.dundee.ac.uk>). As already mentioned above, a nondistinguishable signature was not a factor to rule out the corresponding polar low, as possibly masked by upper clouds. An example of a polar low identified using this detection scheme is shown in the TW field (Figure 1a), wind speed field (Figure 1b), and AVHRR infrared imagery (Figure 1c).

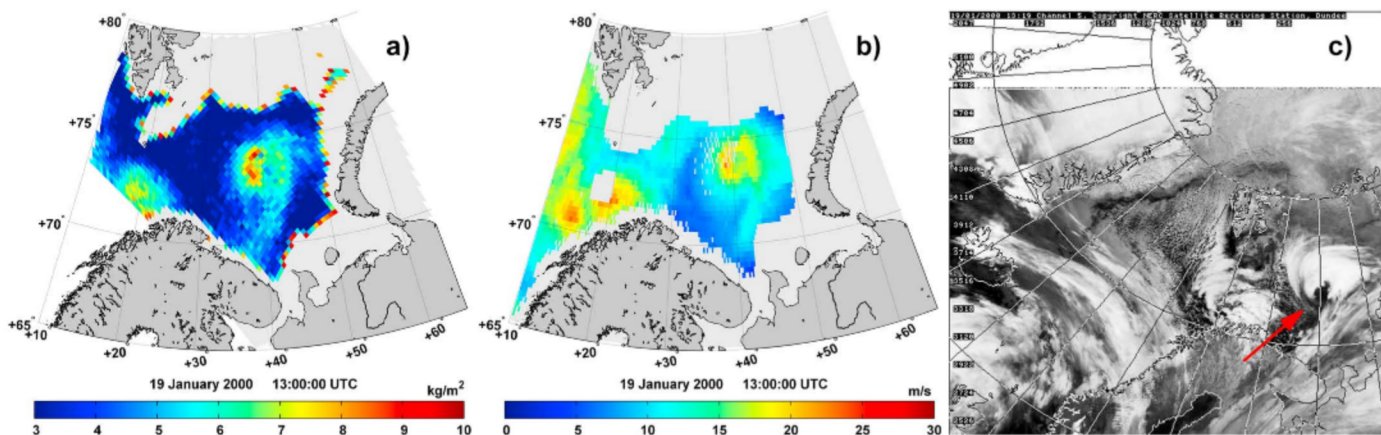


Figure 1. A polar low on 19 January 2000 present on (a) total atmospheric water vapor content field, (b) sea surface wind speed field, and (c) AVHRR thermal infrared imagery; red arrow points to cloud signature associated with a polar low.

For all verified cases, the following parameters were estimated: diameter, lifetime, distance traveled, translation speed, and maximum wind speed. To approximate the diameter of a polar low, we averaged the length of the major and minor axes of an ellipse encompassing polar low signature present in a TW field. All available measurements for a given polar low were then averaged to obtain the mean diameter within its lifetime. The lifetime was initially estimated as the time difference between the last and the first SSM/I observation of a polar low. Then, AVHRR quicklook images were used to improve, when possible, accuracy of estimations as there is a lack of DMSP F13 SSM/I data over the Nordic and Barents seas from 7 P.M. to 3 A.M. due to the orbit of the satellite and SSM/I scanning geometry. The distance traveled was estimated as a sum of distances between successive track points on a polar low trajectory. The translation speed was calculated by dividing the distance traveled by the lifetime derived from SSM/I observations. The maximum wind speed is characterized by the highest wind speed value reached by a polar low during its lifetime.

3. Results

Fourteen extended winter seasons, spanning from September to April, were analyzed. In warm months (from May to August) polar lows are extremely rare and were not considered. From 1995/1996 to 2008/2009, a total of 637 polar lows were detected (45.5 cases per season). Polar low activity exhibits large interseasonal variability (Figure 2a). The maximum number of polar lows is observed in 1999/2000 with 62 events, while only 35 polar

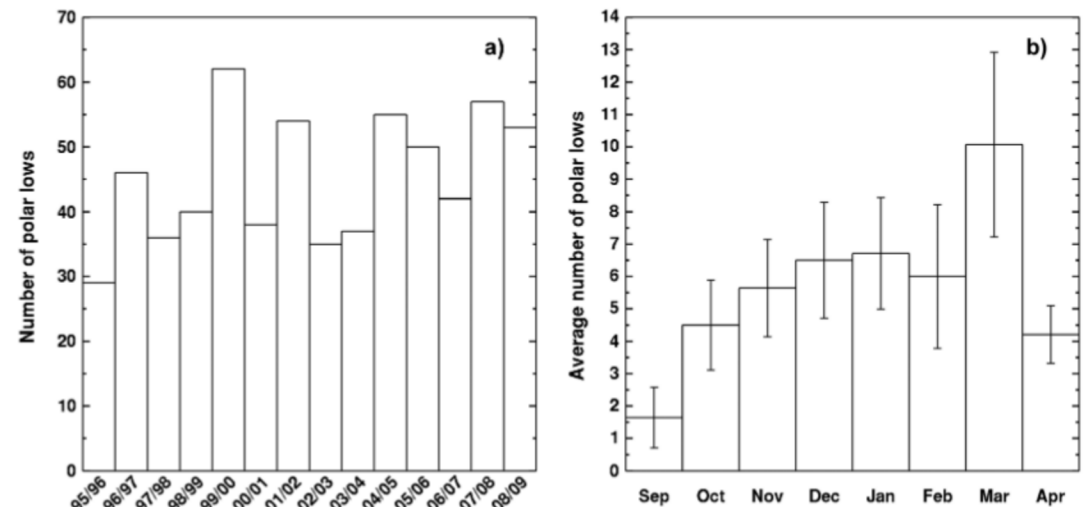


Figure 2. (a) Seasonal and (b) monthly mean frequency distributions of polar lows. Error bars represent corresponding standard deviations.

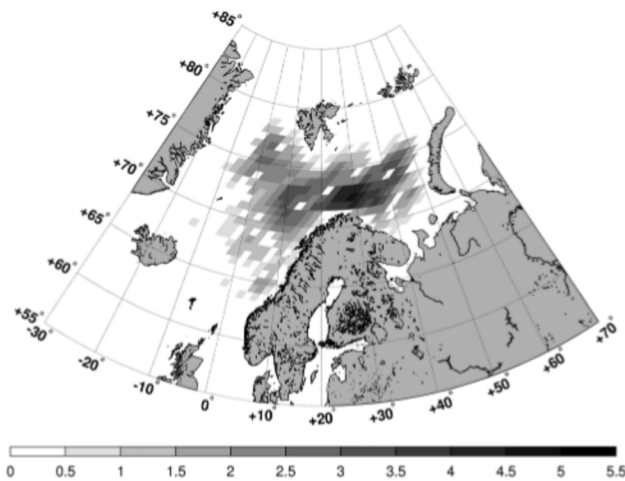


Figure 3. Spatial distribution of detected polar lows over the Nordic seas from September 1995 to April 2009 smoothed by 3×3 cell smoothing window. Units: polar lows per 75×75 km bin cell.

monthly data [Meier et al., 2013] from the National Snow and Ice Data Center (NSIDC) were acquired for September and January of each season to compare polar low frequency and area covered by ice in the Nordic and Barents seas. Sea ice extent calculated with the 10% concentration threshold was used as a measure of the ice area. Low to moderate correlations are obtained between mean sea ice extent in September and the number of polar lows that appeared from September to December of corresponding season ($R=0.34$) and between January mean sea ice extent and number of polar lows from January to April ($R=0.49$). Yet when for the latter case the Barents Sea was solely considered, a high correlation coefficient ($R=0.85$) is found, which is statistically significant at better than the 99.9% significance level. This is also the only case where the null hypothesis of no association between the variables was rejected based on results of the two-tailed *t* test. This clearly demonstrates that decreasing sea ice extent leads to an increase in polar low frequency, and this effect is most discernible in the Barents Sea where the interannual variability of sea ice extent is best pronounced.

Monthly mean frequency distribution of polar lows is shown on Figure 2b. In contrast to other studies where maximum number of polar lows appears in January [e.g., Zahn and von Storch, 2008; Noer et al., 2011], we observe a clear maximum in March with 10.1 polar lows in average. January has the second highest number (6.7 cases). February minimum reported in some previous studies [e.g., Wilhelmsen, 1985; Noer et al., 2011] is not strictly significant in our data set, since the difference between the average numbers, e.g., for February and January, is 0.7, while the standard deviations are 4.4 for February and 3.4 for January. Nevertheless, this is consistent with Noer et al. [2011] where the February minimum is found to be statistically insignificant.

Figure 3 illustrates the spatial distribution of locations where polar lows were first detected binned into 75×75 km cells. Most polar lows (42.5%) formed in the Norwegian Sea. The Barents Sea accounts for 41% of the total number of polar lows; this percentage is much higher than previously reported [Blehschmidt, 2008; Noer et al., 2011]. This might be due to lower temporal resolution for the Barents Sea provided by AVHRR quicklook images used as primary detection tool in some other studies (e.g., for the Norwegian Sea, time interval between consecutive images is 1–4.5 h, while for the Barents Sea it is 3–13 h [Blehschmidt, 2008]). In the Greenland Sea 16.5% of events occurred. The region near the North Cape in the Barents Sea may be distinguished as the main polar low genesis area.

Characteristics of detected polar lows are presented in Figure 4. About half of polar lows are small scale with 200–400 km diameter (Figure 4a). The majority of polar lows do not exceed 500 km in horizontal scale. It should be noted that despite 1000 km diameter was an upper limit for initial selection of polar low-like vortices, none of polar lows exceeded 800 km. Most polar lows existed 9–18 h and only 10% lasted more than 1 day (Figure 4b). Polar lows are found to be quasi-stationary since most of them traveled only 100–300 km (Figure 4c). The majority of polar lows translated at speed within $4\text{--}10\text{ ms}^{-1}$ (Figure 4d).

lows were registered in 2002/2003. A comparison can be done with Blehschmidt [2008] who uses a similar approach (although AVHRR infrared imagery is used instead of microwave data used here) and the same definition of polar lows from Rasmussen and Turner [2003] yet encompasses a slightly larger area (which in addition covers the Irminger Sea) and includes summer months in analysis. For corresponding years, 2004 and 2005, we found 52 and 51 polar lows, respectively, while 51 and 39 events were registered by Blehschmidt [2008].

The Climate Data Record of Passive Microwave Sea Ice Concentration

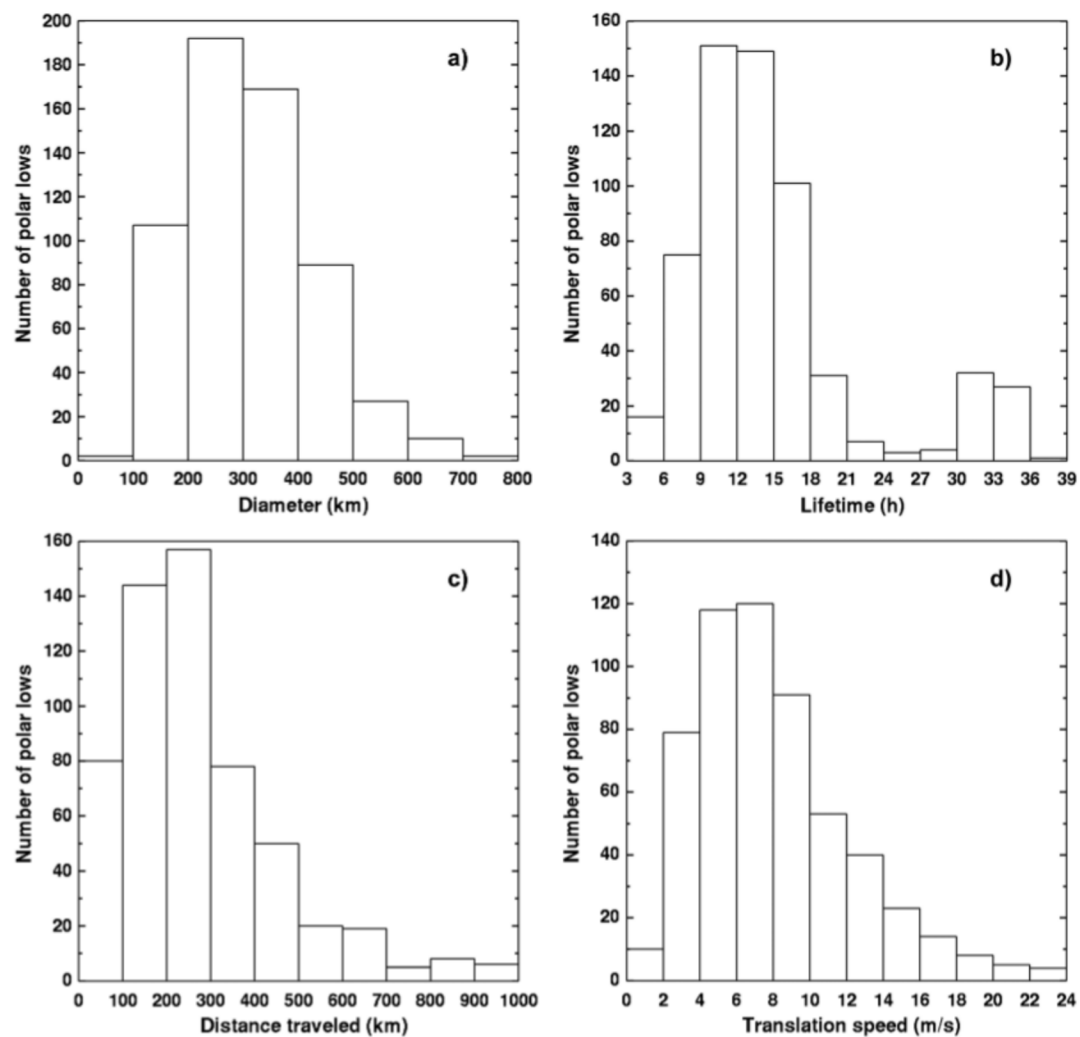


Figure 4. Distribution of polar lows by (a) diameter, (b) lifetime, (c) distance traveled, and (d) translation speed.

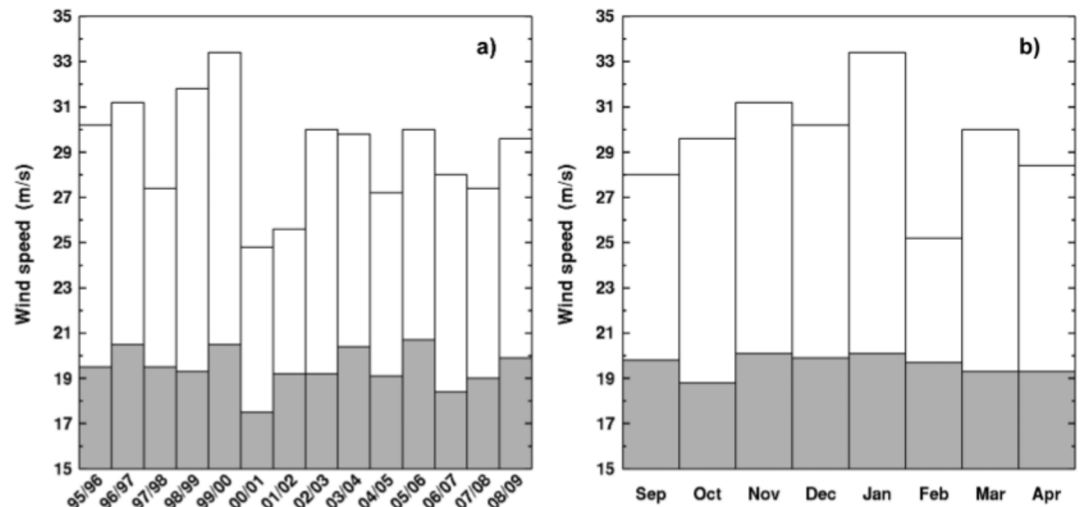


Figure 5. The (a) seasonal and (b) monthly distributions of surface wind speed in detected polar lows. Gray bars represent mean values; white bars depict the highest observed values.

The seasonal and monthly distributions of wind speed in detected polar lows are further shown in Figure 5. In both cases mean values slightly fluctuate near the 19 m s^{-1} mark. The most intense event was observed in January of 1999/2000 season with 33.4 m s^{-1} .

4. Discussion and Conclusions

An approach based on satellite passive microwave data was for the first time adopted for composing a polar low climatology. Polar low-like vortices were first identified in TWW fields. Detected vortices were then confirmed as polar lows if sea surface wind speeds exceeded 15 m s^{-1} , otherwise they were discarded. A total of 637 polar lows were identified over the Nordic seas in 14 seasons (1995/1996–2008/2009), which corresponds to 45.5 cases a season. This number is larger than previously reported in studies based on infrared data. This might be due to the nature of microwaves for which clouds are almost transparent, and thus, information about columnar geophysical parameters of atmosphere may be retrieved. This presents an opportunity to reveal otherwise undetectable polar lows covered by upper clouds.

On the other hand, as discussed in Claud et al. [2009], a polar low climatology solely based on passive microwave data might be biased toward events possessing stronger convection and underestimate number of cases formed as a result of baroclinic instability. This is true for high frequencies where scattering by large ice particles is present. We believe that utilization of lower frequency channels near the water vapor absorption line at 22.235 GHz allowed to avoid this effect in the present results.

Interestingly, frequency in the Barents Sea is comparable to the Norwegian Sea. Together they represent about 83.5% of the total polar low occurrences in the Nordic and Barents seas region. In the Barents Sea, the number of polar lows from January to April is significantly correlated with the January mean sea ice extent, with an increasing occurrence with larger open-water conditions.

As analyzed, the largest number of polar lows is found in March (10.1 on average). In January, which is often reported to be the month with the maximum polar low activity [e.g., Zahn and von Storch, 2008; Noer et al., 2011], 6.7 events on average are found which is the second highest number in the present results.

Indicative polar low characteristics were estimated as follows: the mean diameter is 298 km (standard deviation 110 km), the mean lifetime is 14.7 h (standard deviation 7.7 h), the mean translation speed is 8.1 m s^{-1} (standard deviation 4.2 m s^{-1}), the mean distance traveled is 284 km (standard deviation 213 km), and the mean surface wind speed is 19.6 m s^{-1} (standard deviation 3.6 m s^{-1}).

We note a positive tendency in polar low appearances, which has been estimated as 1.18 cases per season, with March to account for about half of this number. The only other studies assessing tendencies of polar low frequency are based on simulations using reanalysis or model data and find either no trend, i.e., ≈ 0.024 cases per year [Zahn and von Storch, 2008], or even negative trend when considering future changes using Intergovernmental Panel on Climate Change (IPCC) scenarios [Zahn and von Storch, 2010]. As already pointed out, these estimations should be taken with extreme caution since polar lows do not appear in reanalyses to a full extent nor can all of them be captured in simulations. Future studies are certainly required to more carefully evaluate tendency in frequency of polar low genesis.

This letter further illustrates benefits of microwave data which may be used as primary detection tool possessing high reliability especially required in climatological studies. With 14 seasons included, present data set significantly extends existing climatologies and may serve as basis for estimations of polar lows representation in reanalyses.

References

- Blehschmidt, A.-M. (2008), A 2-year climatology of polar low events over the Nordic seas from satellite remote sensing, *Geophys. Res. Lett.*, 35, L09815, doi:10.1029/2008GL033706.
- Bobylev, L. P., E. V. Zabolotskikh, L. M. Mitnik, and M. L. Mitnik (2010), Atmospheric water vapor and cloud liquid water retrieval over the Arctic Ocean using satellite passive microwave sensing, *IEEE Trans. Geosci. Remote Sens.*, 48(1), 283–294, doi:10.1109/TGRS.2009.2028018.
- Bobylev, L. P., E. V. Zabolotskikh, L. M. Mitnik, and M. L. Mitnik (2011), Arctic polar low detection and monitoring using atmospheric water vapor retrievals from satellite passive microwave data, *IEEE Trans. Geosci. Remote Sens.*, 49(9), 3302–3310, doi:10.1109/TGRS.2011.2143720.
- Claud, C., N. M. Mognard, K. B. Katsaros, A. Chedin, and N. A. Scott (1993), Satellite observations of a polar low over the Norwegian Sea by special sensor microwave imager, Geosat, and TIROS-N operational vertical sounder, *J. Geophys. Res.*, 98(C8), 14,487–14,506, doi:10.1029/93JC00650.

Acknowledgments

The authors thank Matthias Zahn and an anonymous reviewer for useful suggestions on improving the manuscript. We thank The Global Hydrology Resource Center (GHRC) (<http://ghrc.nsstc.nasa.gov>) for provision of SSMI TBs. Core support of this research was provided by Russian Federation Government via megagrant 11.G34.31.0078. Support of RFBR grant 12-05-93092, project 14-05-91760-AF_a, Russian Federation Project RFMEFI61014X0006 (agreement 14.610.21.0006), and EU FP7 Project EuRuCAS (agreement 295068) is also acknowledged.

The Editor thanks Matthias Zahn and an anonymous reviewer for their assistance in evaluating this paper.

- Claud, C., G. Heinemann, E. Raustein, and L. McMurdie (2004), Polar low le Cygne: Satellite observations and numerical simulations, *Q. J. R. Meteorol. Soc.*, 130, 1075–1102, doi:10.1256/qj.03.72.
- Claud, C., B. M. Funatsu, G. Noer, and J. P. Chaboureau (2009), Observation of polar lows by the Advanced Microwave Sounding Unit: Potential and limitations, *Tellus, Ser. A*, 61(2), 264–277, doi:10.1111/j.1600-0870.2008.00384.x.
- Laffineur, T., C. Claud, J.-P. Chaboureau, and G. Noer (2014), Polar lows over the Nordic seas: Improved representation in ERA-Interim compared to ERA-40 and the impact on downscaled simulations, *Mon. Weather Rev.*, 142, 2271–2289, doi:10.1175/MWR-D-13-00171.1.
- Meier, W., F. Fetterer, M. Savoie, S. Mallory, R. Duerr, and J. Stroeve (2013), NOAA/NSIDC Climate Data Record of Passive Microwave Sea Ice Concentration, Version 2, 1995–2009, Natl. Snow and Ice Data Cent., Boulder, Colo., doi:10.7265/N55M63M1.
- Noer, G., Ø. Saetra, T. Lien, and Y. Guddal (2011), A climatological study of polar lows in the Nordic Seas, *Q. J. R. Meteorol. Soc.*, 137(660), 1762–1772, doi:10.1002/qj.846.
- Rasmussen, E., and J. Turner (2008), *Polar Lows: Mesoscale Weather Systems in the Polar Regions*, Cambridge Univ. Press, Cambridge, U. K.
- Rojo, M., C. Claud, P. Mallet, G. Noer, A. Carleton, and M. Vicomte (2015), Polar low tracks over the Nordic seas: A 14-winter climatic analysis, *Tellus, Ser. A*, 67, 24660, doi:10.3402/tellusa.v67.24660.
- Wentz, F. J. (1997), A well-calibrated ocean algorithm for special sensor microwave/imager, *J. Geophys. Res.*, 102(C4), 8703–8718, doi:10.1029/96JC01751.
- Wilhelmsen, K. (1985), Climatological study of gale-producing polar lows near Norway, *Tellus, Ser. A*, 37, 451–459, doi:10.1111/j.1600-0870.1985.tb00443.x.
- Zahn, M., and H. von Storch (2008), A long term climatology of North Atlantic polar lows, *Geophys. Res. Lett.*, 35, L22702, doi:10.1029/2008GL035769.
- Zahn, M., and H. von Storch (2010), Decreased frequency of North Atlantic polar lows associated with future climate warming, *Nature*, 467, 309–312, doi:10.1038/nature09388.
- Zappa, G., L. Shaffrey, and K. Hodges (2014), Can polar lows be objectively identified and tracked in the ECMWF operational analysis and the ERA-Interim reanalysis, *Mon. Weather Rev.*, 142, 2596–2608, doi:10.1175/MWR-D-14-00064.1.